Available online at www.sciencedirect.com
SCIENCE DIRECT®
Journal of Sound and Vibration 283 (2005) 243–262
JOURNAL OF SOUND AND VIBRATION
www.elsevier.com/locate/jsvi

On the elastic characterization of composite plates with vibration data

Emmanuel O. Ayorinde*, Lin Yu

Department of Mechanical Engineering, Wayne State University, 5050 Anthony Wayne, Detroit, MI 48202, USA

Received 22 July 1999; accepted 13 April 2004
Available online 25 January 2005

Abstract

This paper takes a global look at a method of obtaining the elastic constants of the material of a rectangular plate sample by explicitly inputting the geometrical shapes and frequencies of a sufficient number of experimental vibration modes into a computational procedure that essentially compares experimental frequencies with analytical predictions. There are many aspects of this method that have important bearing on accuracy, ease of use and computational economy. The issues that arise include vibration representation functions, selection of experimental mode shapes and frequencies for analysis, goodness of experimental data, frequency sensitivity of the elastic constants, influence of diagonal modes where relevant, plate thickness, plate aspect ratio, material orthotropy ratio and orientation of reinforcing fibers in laminate composites. Whereas some of these factors have been discussed separately in other works, this paper attempts bring the method completely into focus in one place, with an examination of all the factors believed to influence the efficiency of the method.

1. Introduction

Composite materials continue to be substituted for more traditional materials in many important segments of the economy, such as the automotive, aerospace, defense and consumer products industries. The main reason for this trend is the superiority of composite materials in the

*Corresponding author. Tel.: +1-313-577-5548; fax: +1-313-577-8789.
E-mail address: aa0983@wayne.edu (E.O. Ayorinde).

0022-460X/$ - see front matter © 2004 Elsevier Ltd. All rights reserved.
doi:10.1016/j.jsv.2004.04.026

areas of specific weight, specific stiffness, and corrosion resistance. Elastic properties, such as stiffness, are of great importance in the engineering design of composite materials. The possibility of tailoring the directional properties of composite materials by manufacturing design makes them very desirable for many purposes, although the possible variation of properties with direction also makes it much harder to identify or characterize a composite material with unknown properties. It is recognized that the "unknown" material may simply be a quantity of the material being quality tested to establish the true properties, as these may have drifted under production conditions. It is also necessary to correctly identify and characterize composite materials to facilitate optimal utilization. Several static methods [1,2] had been established for obtaining the elastic properties of composite materials. Elastic properties are important for composites because these materials are often designed based on stiffness. Disadvantages of static characterization methods, as compared to dynamic methods include being slow, requiring many samples (cut in different orientations) or, with newer methods utilizing single samples, requiring several points of sampling, and being generally more expensive. Vibration-based methods tend to be the least expensive dynamic methods presently utilized.

The vibration method of characterization is basically an optimal curve fitting of vibration test data to some equations expressing the dynamics of the test sample. The use of vibration testing to determine the elastic constants of materials, both isotropic and anisotropic, continues to be widely researched [3–18]. Most of the works are based on thin plate theory with the finite element method or Rayleigh–Ritz method with various forms of assumed field displacements in the forward program.

Ayorinde and Gibson [9] developed a method founded on using Rayleigh's method with the classical lamination theory and a potential-energy-optimized few-modes representation of the transverse displacement of a completely free plate, which representation is itself due to the work of Dickinson and colleagues [19,20,30]. The approach is well documented [8–13], and uses a suitably formed least-squares objective function in the inverse analysis. This approach does not require one to sum over all modes from the fundamental, as is usual with the normal Rayleigh–Ritz and similar methods, but one can specify by frequency and mode shape indices, the precise modes to be included. The mode shape indices represent some function of the numbers of flexural half waves in the orthogonal directions of the plate geometry. In this method, the frequency and mode shape may thus be said to define each mode explicitly, as opposed to several methods where only the frequency is utilized, and the mode identification for comparison is basically implicit. In such methods, which may be described as explicit mode, for example, frequencies of the first so many experimentally obtained modes are compared sequentially in a one-to-one correspondence with those of the first equal number of computed modes, starting from the fundamental. It is absolutely essential in such methods to ensure that no mode is missed out in the sequence on either side (experiment and computation) because this can lead to seriously wrong and even absurd answers [11,14]. With the explicit mode approach, the modes are uniquely identified, by frequency and mode indices. Any number of modes considered adequate for a good solution can then be utilized, chosen in any order, or without order, so long as each time, the experimental and analytical frequencies are being compared for the same particular mode. The work was also customized for an isotropic plate [8], and extended to six optimized modes [10]. A full analysis for a thick orthotropic plate was also developed by Ayorinde [12], using a three-term approximation of displacement.

It is well known that the effects of transverse shear and rotary inertia are important in the flexural vibration of thick plates, and thus, natural frequencies and elastic constants of a thick plate cannot be obtained using the thin plate theory. Some study of flexural vibrations of a rectangular thick plate [21–23] has been conducted, but for completely free edge conditions (which are analytically more difficult, but can be well simulated in experimental tests) relatively few approximate solutions based on thick plate theory and use of finite element methods or Rayleigh methods exist. Both methods have been used [12,15] to obtain the elastic constants of thick plates. Finite element approaches generally require longer solution times than Rayleigh methods, especially with increasing mesh refinement.

The accuracy achieved using Rayleigh methods depends significantly on the goodness of experimental data, as it is clear that poor test results promote mismatches between the analytically predicted and test data. It is proposed in this paper to investigate the severity of the impact of such deviations on the accuracy of predicted elastic constants. This has implications for the quality of the predicted elastic constants, and also on the evaluation of structural integrity, on account of the possible use [28,29] of the frequency values for damage assessment. This issue is treated in the latter part of this paper.

Square, isotropic plates in transverse vibration manifest some coupled modes called "diagonal modes" caused by the symmetry of boundary conditions and geometry about a diagonal [20,24–27]. These modes comprise the sums and the differences of pure, indicially inverse modes such as (i,j) and (j,i), and are therefore described as $(i,j\pm j,i)$ modes. In the earlier works by Ayorinde and colleagues, in order to avoid more complexity, the "diagonal modes" were skipped from the displacement representations when square, isotropic or almost isotropic plates with free boundary conditions were dealt with. However, in a more recent work [13], Ayorinde and Yu analyzed these modes and included them in the identification problem. Diagonal modes are also examined in this paper.

The issue of the sensitivity of these modes to the elastic constants will also be addressed in this paper, since the accuracy of the elastic identification problem is very dependent on these sensitivities. It should be noted that the diagonal modes are automatically included if one utilizes the Rayleigh–Ritz method with a sufficient number of the lower terms in the series representation of the deformation [6,19,26]. The diagonal modes are also automatically analyzed when the finite element method is utilized. When using explicit mode methods like the improved Rayleigh method introduced by Kim and Dickinson [20], however, the diagonal modes should be inserted into the normal expression of displacement.

The use of sensitivity analysis in the identification of elastic constants of composite materials was also contemplated by several workers [7,14,11,31–34]. It is logical that, on account of inevitable variations between the predictions of the analytical model and the practical experiment, consideration of the frequency sensitivities with respect to the elastic constants be linked to the identification of elastic properties of materials, and should be helpful in selecting the best modes for use in such an exercise.

In the present approach, the vibration frequencies are first estimated from the plate vibration model and known elastic constants, in what is termed the "forward" problem. The degree of ease of solution of this forward problem and the accuracy of its solution provide an indication of the feasibility and relative ease of solution of the "inverse" problem, which is the identification of elastic constants from experimental vibration data. Sensitivity analysis is included in both the

"forward" and "inverse" problems as well. The best (in the sense of having the highest sensitivities) mode set for each elastic constant is automatically selected from the input experimental vibration data.

The rectangular geometry plate sample is usually the easiest to prepare, and is therefore most often utilized in the identification exercise. The completely free boundary condition is also normally utilized because it is the most accurately realizable in practice. Accordingly, all our work to date is based on these conditions.

In the authors' work, modal frequency parameters and the frequency sensitivity parameters of the elastic constants have been studied for fiber angle variations between 0° and 90°. Completely free rectangular plates of varying aspect ratios, fiber angle orientations, material orthotropy ratios, and cross-ply lay-up are examined. These are important considerations in the procedures currently widely applied for the elastic identification and damage analysis of composite materials.

2. Analysis

2.1. General

The procedure followed by the authors in this study has been documented by Ayorinde and colleagues [8–10,12]. For the sake of completeness, a basic description of the theory and procedure is given here.

For a symmetrically laminated rectangular plate at equilibrium in the xy-plane, the free transverse vibration equation may be written as

$$D_{11}\frac{\partial^4 w}{\partial x^4} + 4D_{16}\frac{\partial^4 w}{\partial x^3 \partial y} + 2(D_{12} + 2D_{66})\frac{\partial^4 w}{\partial x^2 \partial y^2} + 4D_{26}\frac{\partial^4 w}{\partial x \partial y^3} + D_{22}\frac{\partial^4 x}{\partial y^4} + \rho\, h\frac{\partial^2 w}{\partial t^2} = 0, \tag{1}$$

where the plate transverse deflection is $w(x,y,t)$, x and y are the orthogonal plate coordinates, D_{ij} is the standard bending stiffness of the classical lamination theory, ρ is the plate density, h is the plate thickness and t represents time. For specially orthotropic plates, $D_{16} = D_{26} = 0$, $D_{11} = D_x$, $D_{22} = D_y$, $D_{12} = v_{xy}\, D_y$ and $D_{66} = D_{xy}$, where $D_x = E_x h^3/12(1 - v_{xy}v_{yx})$, $D_y = E_y D_x/E_x$, $D_{xy} = h^3 G_{xy}/12$. Since the isotropic plate is a particular case of the orthotropic plate, the equilibrium equation for the isotropic plate is simpler and can be obtained from eq. (1) simply by replacing v_{xy} and v_{yx} with v, D_x and D_y with $D = Eh^3/12(1-v^2)$, and $2D_{xy} = 2(3-v)D$, where E is Young's modulus and v is the Poisson ratio.

For a typical diagonally symmetrical mode the expressions for transverse displacement, for the six-mode representation, could be adequately represented by the expression

$$W(x,y) = A\Big\{\Big(\theta_i\phi_j - c\theta_i\phi_n - d\theta_m\phi_j - e\theta_i\phi_q - f\theta_m\phi_n - g\theta_p\phi_j\Big) \pm \Big(\theta_j\phi_i - c\theta_n\phi_i - d\theta_j\phi_m - e\theta_q\phi_i - f\theta_n\phi_m - g\theta_j\phi_p\Big)\Big\}, \tag{2}$$

where the mode shape of interest is the (i, j)th, A, c, d, e, f and g are constants, θ is a function of x and ϕ is a function of y. $\theta_i(x)$ and $\phi_j(y)$ are the appropriate ith and jth beam mode shapes, $m = i + 1$, $p = i + 2$, $n = j + 1$, $q = j + 2$ for dissimilar beam ends and $m = i + 2$, $p = i + 4$, $n = j + 2$, $q = j + 4$ for the case where the conditions are the same at each end. It may be noted that the items in the first small bracket on the right hand side of Eq. (2) constitute the expression for the normal six modes. And the diagonal one-term displacement expression, suggested by Warburton [25] and examined by Kim and Dickinson [20], is taken as a simple truncation of the above by letting $c = d = e = f = g = 0$. The corresponding three-mode expressions can be obtained by setting $e = f = g = 0$.

The maximum kinetic and potential energy expressions, respectively, are given by

$$T_{\max} = \frac{1}{2}\rho h\omega^2 \int_0^a \int_0^b W^2 \,\mathrm{d}x\mathrm{d}y \tag{3}$$

and

$$V_{\max} = \frac{1}{2}\int_0^a \int_0^b D_x \left\{ \left(\frac{\partial^2 W}{\partial x^2}\right)^2 + 2v_{xy}D_y \frac{\partial^2 W}{\partial x^2}\frac{\partial^2 W}{\partial y^2} + D_y\left(\frac{\partial^2 W}{\partial y}\right)^2 + 4D_{xy}\left(\frac{\partial^2 W}{\partial x \partial y}\right)^2 \right\} \mathrm{d}x\,\mathrm{d}y, \tag{4}$$

where ω is the frequency of vibration, and a and b are the plate side dimensions along the x- and y-axis. After substituting the displacement expression (2) into Eqs. (3) and (4), we may have

$$T_{\max} = A^2\rho h\omega^2\left(1 + c^2 + d^2 + e^2 + f^2 + g^2\right)X_i Y_j, \tag{5}$$

$$\begin{aligned} V_{\max} = \frac{A^2 H\pi^4}{a^2 b^2}\{ & C_{ij} + c^2 C_{in} + d^2 C_{mj} + e^2 C_{iq} + f^2 C_{mn} + g^2 C_{pj} - 2cE_{ij} - 2dE_{ji} - 2eE_{ij^*} \\ & - 2fQ_{ji} - 2gE_{ji^*} + 2cdF_{ij} + 2ceE_{in} + 2cfE_{ni} + 2cgF_{i^*j} + 2deF_{ij^*} + 2dfE_{mi} \\ & + 2dgE_{jm} + 2efF_{in} + 2egF_{i^*j^*} + 2fgF_{mj}\}X_i Y_j, \end{aligned} \tag{6}$$

where

$$X_i = \int_0^a \theta_i^2 \mathrm{d}x, \quad Y_j = \int_0^b \phi_j^2 \mathrm{d}y, \quad H = v_{xy}D_y + 2D_{xy} \tag{7}$$

and

$$\begin{aligned} C_{ij} &= (D_x/H)G_i^4(b^2/a^2) + (D_y/H)G_j^4(a^2/b^2) + 2[H_iH_j + (D_{xy}/H)(J_iJ_j - H_iH_j)], \\ E_{ij} &= H_i(K_j + L_j)[2(D_{xy}/H) - 1] + 4(D_{xy}/H)J_iM_j, \\ F_{ij} &= -(K_iK_j + L_iL_j)[2(D_{xy}/H) - 1] + 4(D_{xy}/H)M_iM_j, \\ Q_{ij} &= -(K_jL_i + K_iL_j)[2(D_{xy}/H) - 1] + 4(D_{xy}/H)M_iM_j. \end{aligned} \tag{8}$$

For the isotropic square plates, where diagonal modes would occur,

$$C_{ij} = C_{ij} \pm \bar{C}_{ij}, \quad E_{ij} = E_{ij} \pm \bar{E}_{ij}, \quad F_{ij} = F_{ij} \pm \bar{F}_{ij}, \quad Q_{ij} = Q_{ij} \pm \bar{Q}_{ij}, \tag{9–12}$$

where the coefficients under the bar are diagonal mode related terms. The coefficients are given by

$$\begin{aligned}
C_{ij} &= G_i^4 + G_j^4 + 2[\nu H_i H_j + (1-\nu) J_i J_j], & \bar{C}_{ij} &= \nu(K_{ij}^2 + K_{ji}^2) + 2(1-\nu) M_{ij}^2,\\
E_{ij} &= -\nu(K_j + L_j) H_i + 2(1-\nu) J_i M_j, & \bar{E}_{ij} &= \nu(K_{ij} K_{in} + K_{ji} K_{ni}) + 2(1-\nu) M_{ij} M_{in},\\
E_{ji} &= -\nu(K_i + L_i) H_j + 2(1-\nu) J_j M_i, & \bar{E}_{ji} &= \nu(K_{ji} K_{mj} + K_{ij} K_{mj}) + 2(1-\nu) M_{ji} M_{mj},\\
F_{ij} &= \nu(K_i K_j + L_i L_j) + 2(1-\nu) M_i M_j, & \bar{F}_{ij} &= \nu(K_{ij} K_{mn} + K_{ji} K_{nm}) + 2(1-\nu) M_{ij} M_{mn},\\
Q_{ij} &= \nu(K_j L_i + K_i L_j) + 2(1-\nu) M_i M_j, & \bar{Q}_{ij} &= \nu(K_{in} K_{mj} + K_{ni} K_{jm}) + 2(1-\nu) M_{in} M_{jm}.
\end{aligned} \tag{13}$$

The integrals G_i, H_i, J_i, K_i, L_i, M_i and K_{ij}, M_{ij} are based on normal-mode free–free beam characteristic functions, and are given by

$$\begin{aligned}
G_i^4 &= \left(a^4/\pi^4\right) \int_0^a (\theta_i'')^2 \,\mathrm{d}x \Big/ \int_0^a \theta_i^2 \,\mathrm{d}x,\\
H_i &= -\left(a^2/\pi^2\right) \int_0^a \theta_i \theta_i'' \,\mathrm{d}x \Big/ \int_0^a \theta_i^2 \,\mathrm{d}x,\\
J_i &= \left(a^2/\pi^2\right) \int_0^a (\theta_i'')^2 \,\mathrm{d}x \Big/ \int_0^a \theta_i^2 \,\mathrm{d}x,\\
K_i &= \left(a^2/\pi^2\right) \int_0^a \theta_i \theta_m'' \,\mathrm{d}x \Big/ \int_0^a \theta_i^2 \,\mathrm{d}x,\\
L_i &= \left(a^2/\pi^2\right) \int_0^a \theta_i'' \theta_m \,\mathrm{d}x \Big/ \int_0^a \theta_i^2 \,\mathrm{d}x,\\
M_i &= \left(a^2/\pi^2\right) \int_0^a \theta_i' \theta_m \,\mathrm{d}x \Big/ \int_0^a \theta_i^2 \,\mathrm{d}x,\\
K_{ij} &= \left(a^2/\pi^2\right) \int_0^a \theta_i \theta_j'' \,\mathrm{d}x \Big/ \int_0^a \theta_i^2 \,\mathrm{d}x,\\
M_{ij} &= \left(a^2/\pi^2\right) \int_0^a \theta_i' \theta_j' \,\mathrm{d}x \Big/ \int_0^a \theta_i^2 \,\mathrm{d}x.
\end{aligned} \tag{14}$$

In the above equations, $m = i + 2$. The y-direction integrals, such as G_j, H_j, etc. are obtained by substituting function $\phi_{(y)}$, indices j and n for $\theta_{(x)}$, i and m, respectively, in the previous equations. The constants with the bar in Eq. (7) and the integrals K_{ij} and M_{ij} in Eq. (8) are caused by the diagonal modes. The asterisked constants in Eq. (6), only for the case of the use of the six-mode displacement expression, are the versions of the constants that utilize differently incremented indices. These constants may be obtained by simply substituting i^* or j^* with i and j, respectively, in Eq. (7), and the related integrals are typically given by

$$\begin{aligned}
K_{i^*} &= \left(a^2/\pi^2\right) \textstyle\int_0^a \theta_i \theta_p'' \,\mathrm{d}x \Big/ \int_0^a \theta_i^2 \,\mathrm{d}x,\\
L_{i^*} &= \left(a^2/\pi^2\right) \textstyle\int_0^a \theta_p'' \theta_p \,\mathrm{d}x \Big/ \int_0^a \theta_i^2 \,\mathrm{d}x,\\
M_{i^*} &= \left(a^2/\pi^2\right) \textstyle\int_0^a \theta_i' \theta_p' \,\mathrm{d}x \Big/ \int_0^a \theta_i^2 \,\mathrm{d}x.
\end{aligned} \tag{15}$$

Here, $p=i+4$. Constants c, d, e, f, and g are obtained by optimizing the potential energy with respect to each one of them (i.e. $\partial V_{\max}/\partial z = 0$, for $z=c$, d, e, f, and g, respectively). This yields in matrix form

$$[A]x = b, \tag{16}$$

where

$$[A] = \begin{bmatrix} C_{in} & F_{ij} & E_{in} & E_{ni} & F_{i^*j} & \\ & C_{mj} & F_{ij^*} & E_{mj} & E_{jm} & \\ & & & C_{iq} & F_{in} & F_{i^*j^*} \\ & \text{Sym} & & & C_{mn} & F_{mj} \\ & & & & & C_{pj} \end{bmatrix}, \quad x = \begin{Bmatrix} c \\ d \\ e \\ f \\ g \end{Bmatrix} \quad \text{and} \quad b = \begin{Bmatrix} E_{ij} \\ E_{ij} \\ E_{ij^*} \\ Q_{ij} \\ E_{ij^*} \end{Bmatrix}. \tag{17}$$

When the maximum values of the kinetic and potential energies [Eqs. (5) and (6)] are equated according to Rayleigh's method, the explicit frequency equation is obtained as

$$\begin{aligned} \frac{\rho h a^2 b^2}{\pi^4} = \frac{H}{\omega^2(1+c^2+d^2+e^2+f^2+g^2)} * \big[& C_{ij} + c^2 C_{in} + d^2 C_{mj} + e^2 C_{iq} + f^2 C_{mn} + g^2 C_{pj} \\ & - 2cE_{ij} - 2dE_{ji} - 2eE_{ij^*} - 2fQ_{ij} - 2gE_{ji^*} + 2cdF_{ij} + 2ceE_{in} + 2cfE_{ni} \\ & + 2cgF_{i^*j} + 2deF_{ij^*} + 2dfE_{mj} + 2dgE_{jm} + 2efF_{in} + 2egF_{i^*j^*} + 2fgF_{mj} \big], \end{aligned} \tag{18}$$

where $H = v_{xy}D_y + 2D_{xy}$. As mentioned before, $C_{ij} = C_{ij} \pm \bar{C}_{ij}$, $E_{ij} = E_{ij} \pm \bar{E}_{ij}$, $F_{ij} = F_{ij} \pm \bar{F}_{ij}$ and $Q_{ij} = Q_{ij} \pm \bar{Q}_{ij}$ for the isotropic square plates in the above equations. It may be noted that the procedure mentioned earlier for obtaining the one-term approximation essentially leads to setting $c=d=e=f=g=0$ in Eqs. (16) and (18). Similarly, that for the three-term approximation leads to setting $e=f=g=0$.

According to the reasoning advanced in Ref. [9], we also regard the above equation as involving two functions, one of which (the left hand side of Eq. (18)) may be exactly evaluated from geometrical and material density properties, and the other (the right hand side of Eq. (18), only approximately, from measurements. This equation may be written as

$$f_L = f_R(\omega). \tag{19}$$

Then the residual function, in dimensionless form, may be taken as

$$R_Q = \sum_{i=1}^{4} \left[\left(\frac{f_R}{f_L} - 1 \right)^2 \right]_i. \tag{20}$$

This residual function is used as the objective function. The summation is from 1 to 4 in this particular equation because four frequency equations are required to obtain the four independent elastic constants associated with the thin orthotropic plate. In general, the summation would be done to the number of unknown elastic constants that are being sought. For the purely isotropic plates, although two frequency equations are sufficient to obtain the only two unknown constants, the full orthotropic approach is normally followed for the prediction of the elastic constants of isotropic materials to avoid prior presumption of perfect isotropy, which may in fact not hold, for a variety of reasons including manufacturing uncertainties.

2.2. Thick plates

As the plates or panels being tested or analyzed get thicker, and through-the-thickness shear and rotary inertia begin to be important, the Euler–Bernoulli model no longer suffices to adequately describe motion. A significant problem is that the solution of the frequency equation, which is now much more complicated on account of these factors now requires much more computing resources. Since the full inverse problem requires numerous iterative trial solutions, the computational resources required can quickly become very costly. In order to apply the outlined characterization method to a thick plate with no significant increase in computer time and storage, it is essential to develop methods of speeding up the process for such cases.

Starting with the three-mode expression, the transverse deflection $W(x,y)$ of a plate whose mean position lies wholly in the x–y plane may be rendered [20] as

$$W_{ij}(x,y) = A\theta_i(x)\phi_j(y) - C\theta_i(x)\phi_n(y) - D\theta_m(x)\phi_j(y). \tag{21}$$

The bending slopes of the plate along the x-direction $\psi_x(x,y)$ and y-direction $\psi_y(x,y)$ may be respectively written as [12,35]

$$\begin{aligned} \psi_x(x,y) &= B\eta_i(x)\phi_j(y) - G\eta_i(x)\phi_n(y) - P\eta_m(x)\phi_j(y), \\ \psi_x(x,y) &= Z\theta_i(x)\gamma_j(y) - Q\theta_i(x)\gamma_j(y) - V\theta_i(x)\gamma_j(y), \end{aligned} \tag{22}$$

where $\theta(x)$ and $\phi(y)$ are the deflections of beams lying wholly along the x- and y-directions respectively, $\eta(x)$ is the bending slope of the beam when taken as a strip of the plate along the x-axis; and $\gamma(y)$ is the similar slope along the y-direction.

From the foregoing, the potential energy expression becomes

$$\begin{aligned} \mathrm{PE}_{\max} = \iint & [D_{11}\{B\eta_i'(x)\phi_j(y) - G\eta_i'(x)\phi_n(y) - P\eta_m'(x)\phi_j(y)\}^2 \\ & + D_{22}\{Z\theta_i(x)\gamma_j'(y) - Q\theta_i(x)\gamma_n'(y) - V\theta_m(x)\gamma_j'(y)\}^2 + 2D_{12}\{B\eta_i'(x)\phi_j(y) \\ & - G\eta_i'(x)\phi_n(y) - P\eta_m'(x)\phi_j(y)\}\{Z\theta_i(x)\gamma_i'(y) - Q\theta_i(x)\gamma_n'(y) \\ & - V\theta_m(x)\gamma_j'(y)\} + D_{66}\{B\eta_i'(x)\phi_j(y) - G\eta_i'(x)\phi_n(y) - P\eta_m'(x)\phi_j(y) \\ & + Z\theta_i(x)\gamma_j'(y) - Q\theta_m(x)\gamma_n'(y) - V\theta_m(x)\gamma_j'(y)\} + A_{44}\{Z\theta_i(x)\gamma_j(y) \\ & - Q\theta_i(x)\gamma_n(y) - V\theta_m(x)\gamma_j(y) + A\theta_i(x)\phi_j'(y) - C\theta_i(x)\phi_n'(y) \\ & - D\theta_m(x)\phi_j'(y)\}^2 + A_{55}\{B\eta_i(x)\phi_j(y) - G\eta_i(x)\phi_n(x) - P\eta_m(x)\phi_j(y) \\ & + A\theta_i'(x)\phi_j(y) - C\theta_i'(x)\phi_n(y) - D\theta_m'(x)\phi_j(y)\}^2]\,\mathrm{d}y\,\mathrm{d}x. \end{aligned} \tag{23}$$

From an optimization of the potential energy, the nine undetermined constants A, B, C, D, G, P, Z, Q and V may be obtained [11]. Also, the vibration frequency of the plate can then be computed by substituting the nine constants into the expressions for $\mathrm{P.E.}_{\max}$ and $\mathrm{K.E.}_{\max}$. Finally, for each mode, the frequency is obtained using the Rayleigh formula, as

$$\omega^2 = \mathrm{P.E.}_{\max}/\mathrm{K.E.}_{\max}. \tag{24}$$

The plate vibration is essentially constituted from the normal mode vibrations of beam strips lying wholly along the two axial directions of the plate. The solution acceleration artifice which

was found successful, and was utilized in this work, consisted of setting up and using a thick beam normal mode vibration library as an interpolation base, and then utilizing the beam normal modes in synthesizing the plate vibration. Further information on the approach will be given later in the paper.

2.3. Influence on frequency parameter

The modal frequency is quite important in the current approach to characterizing composite materials, as most methods essentially compare a sequenced number of analytical frequencies to their experimental counterparts. Errors in the values or sequences of these frequencies can therefore seriously compromise the accuracy of results.

It is therefore useful to examine the effects of basic parameters like orthotropy ratio, plate aspect ratio, and fiber orientation on modal frequency. Such an examination is made in this paper. The frequency parameter is taken essentially as a scaled eigenvalue, and is here defined as

$$R_{ij} = \omega_{ij} a^2 \left(\frac{\rho}{E_2 h^3} \right)^{1/2}, \tag{25}$$

where ω_{ij} is the frequency of the (i,j)th mode, a is the length of the major side of the sample (plate aspect ratio is defined here as a/b, and is increased by shortening b), ρ is the mass density, h is the sample thickness, and E_2 is Young's modulus in the transverse direction of the sample.

2.4. Sensitivity

The frequency sensitivity of the elastic constants varies widely across the vibration modes. This is the reason why it has been observed [11,18] that different modal data combinations could give very different predictions of the same elastic constants, from the totally unacceptable to the virtually exact sometimes. The issue of sensitivity is therefore very important to the success of the characterization method, and should be considered. Generally, sensitivity should be integrated into the algorithm wherever feasible.

In order to find the influence of a utilized frequency on a derived elastic constant, we may use the proportional change in the frequency for a given proportional change in the elastic constant as the definition of the sensitivity of the mode, for example, for E_x, the sensitivity S_{ω/E_x} is $(\delta\omega/\omega)/(\delta E_x/E_x)$. This may be rearranged as

$$S_{\omega/E_x} = \frac{\partial\omega/\partial E_x}{\omega/E_x}. \tag{26}$$

Similar expressions may be written for the other elastic constants. Since Eq. (12) gives the frequency explicitly, it may be differentiated with respect to each elastic constant to obtain any desired sensitivity. The sensitivity formulation concerning the diagonal modes may be obtained by replacing the C_{ij}, E_{ij}, F_{ij}, and Q_{ij} with $C_{ij} = C_{ij} \pm \bar{C}_{ij}$, $E_{ij} = E_{ij} \pm \bar{E}_{ij}$, $F_{ij} = F_{ij} \pm 0\bar{F}_{ij}$ and $Q_{ij} = Q_{ij} \pm \bar{Q}_{ij}$, respectively, in that reference. The relative derivatives concerning the diagonal modes

are obtained from these. For example, for E_x:

$$\begin{aligned}
\partial \bar{C}_{ij}/\partial E_x &= 2(2M_{ij}^2 - K_{ij}^2 - K_{ji}^2)\partial(D_{xy}/H)/\partial E_x,\\
\partial \bar{E}_{ij}/\partial E_x &= 2(2M_{ij}M_{in} - K_{ij}K_{in} - K_{ji}K_{ni})\partial(D_{xy}/H)/\partial E_x,\\
\partial \bar{C}_{ij}/\partial E_x &= 2(2M_{ij}M_{nm} - K_{ij}K_{mn} - K_{ji}K_{nm})\partial(D_{xy}/H)/\partial E_x.
\end{aligned} \tag{27}$$

In the case of the application of the three-term approximation, the constants c and d can be expicitly solved for in terms of the coefficients C_{ij}, E_{ij} and F_{ij} or $C_{\mathrm{ij}} \pm \bar{C}_{ij}$, $E_{ij} \pm \bar{E}_{ij}$, and $F_{ij} \pm \bar{F}_{ij}$, and thus their derivatives with respect to elastic constants can be obtained directly. When the six-term displacement expression is used, however, the constants c, d, e, f and g are implicitly determined by the matrix equation (16) and their derivatives, for example with respect to E_x, may be obtained by solving a set of linear equations as in the following:

$$\partial x/\partial E_x = [A]^{-1}\{\partial b/\partial E_x - (\partial[A]/\partial E_x)x\}. \tag{28}$$

2.5. Goodness of experimental data

No matter how rigorous the analytical and computational formulations are, it may easily be inferred that the practical limitation on accuracy is the goodness of the input experimental data. Some investigation of how this works out is made in this paper. The effects of using input modal data that are perturbed a little from the theoretically accurate values, and the degrees of deviation of predicted elastic constants from the expected values are obtained and examined.

3. Procedure

The sensitivity analysis is included in both the "forward" and "inverse" problems. In this way the best set of experimental modes is utilized to back out elastic constants based on the experimental modal data.

The "inverse" problem of estimating the elastic constants from experimental modal data is then solved with the displacement expression including the diagonal modes. The basic optimization procedure described in the original work [9] is followed. The practical application of this method may be done in a variety of ways. One may use the lowest several experimental frequencies, which have the advantage of being more accurately obtainable in practice than the higher modes, as the input data into the inverse program. From this scheme, the optimal value of each elastic constant is then obtained with the least residual in the final search.

4. Results

The single-, three- and six-mode displacement expressions are utilized first in the "forward" problem of obtaining the natural frequencies of plates with given geometric and elastic constants, and the possibility of having diagonal modes is included in the analysis. Frequencies are obtained

by solving the frequency equation (18) for ω with the appropriate modal shape indices. Various samples were used in the experimental part of the work. These included isotropic square plates made of aluminum and SMC materials and the orthotropic square plates made of *E*-glass/epoxy and graphite/epoxy materials. The aluminum plate measured 254 mm × 254 mm × 3.16 mm and had a mass/unit volume density of 2770 kg/m^3. The Sheet Molding Compound (SMC) had randomly oriented chopped glass fibers in a polyester matrix and had a density of 1850 kg/m^3 and the SMC plate measured 306 mm × 305.6 mm × 2.682 mm. The 12-ply graphite/epoxy plate measured 254 mm × 254 mm × 1.483 mm and had a density of 1540 kg/m^3.

Table 1 compares the values of a dimensionless frequency parameter as obtained by Blevins [27] and also by our method. Table 2 gives the sequences of the lowest four modes for a graphite/

Table 1
Dimensionless frequency parameter λ_{ij}^2 ($v = 0.3$)

	Mode indices					
	(2,2)	(3,1−1,3)	(1,3 + 3,1)	(3,2)	(2,3)	(4,1)
Blevins' data[a]	13.49	19.79	24.43	35.02	35.02	61.53
Aluminum plate results[b]	13.61[0.9][c]	19.81[0.1]	24.46[0.1]	35.54[1.5]	35.54[1.5]	61.63[0.2]
SMC plate results[b]	13.69[1.5]	19.79[0.0]	24.47[0.2]	35.67[1.8]	35.67[1.8]	61.63[0.2]

Note: $\lambda_{ij}^2 = \omega_{ij} \cdot 2\pi a^2 \left[\frac{Eh^3}{12\rho(1-v^2)}\right]^{-1/2}$.
[a]From Blevins [27].
[b]From the three-mode approximation with diagonal modes.
[c][ ] contain the percent difference from the Blevins' data.

Table 2
Plate modal sequences for graphite/epoxy

	Lowest four-mode sequence
Rectangular plate	
0° *Fiber orientation*	
Plate aspect ratio	
1	(2,2),(1,3),(2,3),(1,4)
2	(2,2)(3,1),(1,3),(3,2)
3	(2,2)(3,1),(3,2),(1,3)
4	(2,2)(3,1),(3,2),(4,1)
Square plate	
Fiber orientation	
0°	(2,2),(1,3),(2,3),(1,4)
15°	(2,2),(1,3),(2,3),(3,1)
30°	(2,2),(1,3),(3,1),(2,3)
45°	(2,2),(3,1),(1,3),(3,2)
60°	(2,2),(3,1),(1,3),(3,2)
75°	(2,2),(1,3),(3,2),(1,3)
90°	(2,2),(3,1),(3,2),(4,1)

Note: Rectangular plate of sides *a*, *b*; aspect ratio, *a*/*b*, varied by changing *b*.

Table 3
Natural frequencies of square SMC plate with completely free boundary conditions

Modal indices	Natural frequencies (Hz)					
	Exptl.	One-mode with diag.	Three-mode with diag.	Six-mode with diag.	36-term R.-R[a]	64-term R.-R[a]
2,2	54.4[−2.1][b]	58.59[5.5]	55.92[0.7]	55.65[0.20]	55.56[0.04]	55.54
3,1−1,3	78.8[−2.75]	81.73[−0.86]	81.35[0.40]	81.10[0.09]	81.22[0.23]	81.03
1,3 + 3,1	99.2[0.90]	99.02[0.71]	98.53[0.21]	98.40[0.08]	98.47[0.15]	98.32
2,3	138.4[−3.42]	149.69[4.46]	145.15[1.29]	144.82[1.06]	143.50[0.14]	143.30
3,2	138.4[−3.42]	149.69[4.46]	145.15[1.29]	144.82[1.06]	143.50[0.14]	143.30
1,4	242.4[−2.76]	250.17[0.36]	249.98[0.28]	249.83[0.22]	249.64[0.15]	249.27
4,1	242.4[−2.76]	250.17[0.36]	249.98[00.28]	249.83[0.22]	249.64[0.15]	249.27
3,3	254.0[−3.02]	276.23[5.47]	264.19[0.87]	262.86[0.37]	263.34[0.55]	261.90
2,4−4,2	263.4[−7.81]	285.86[0.06]]	285.83[0.05]	285.75[0.02]	285.77[0.03]	285.70
4,2 + 2,4	306.6[−2.72]	325.23[3.26]	315.58[0.20]	314.77[−0.06]	315.37[0.13]	314.96

[a]From Deobald and Gibson [6].
[b][ ] contain % difference from 64-term Rayleigh–Ritz data

epoxy plate as the plate aspect ratio is varied, and for a square planform, as the unidirectional fiber orientation is varied. Table 3 shows the natural frequencies of a square SMC plate, using different numbers of terms in approximating the displacement function. Fig. 1 shows the frequency sensitivities of the elastic constants of a square SMC plate for several modes. Table 4 shows a typical result of the attempt to find a global fit for the plate frequencies based on material and geometric parameters. Fig. 2 displays the computation times for the forward problem for thick graphite/epoxy plates, comparing and contrasting the use of the interpolation library. Fig. 3 shows the effect of plate aspect ratio on the frequency parameter of glass/epoxy with 0° fiber orientation. Fig. 4 shows the effect of fiber orientation on the frequency sensitivity of an elastic constant, the Poisson's ratio. Table 5 is a sample detail of the errors introduced into the extracted elastic constants by using as input experimental frequencies that are in error to specified extents. In this case, a mode, (4,1) has high sensitivity to the transverse Young's modulus, E_y. The contribution of this mode to the accuracy of the modulus E_y is therefore significant. It may therefore be expected that if this mode should be incorrectly measured or input, the predicted value of E_y would be correspondingly in error. Table 5 gives numerical values for this sample case.

5. Discussion

The data and diagrams in this paper are only a sample of the quantum of results obtained in the authors' research being overviewed, but an attempt is made to discuss the salient points of important observations.

The values of a dimensionless frequency parameter as obtained by Blevins [27] are compared in Table 1 to those obtained by our method for aluminum and the composite material SMC. The good agreement suggests that our approach has high accuracy.

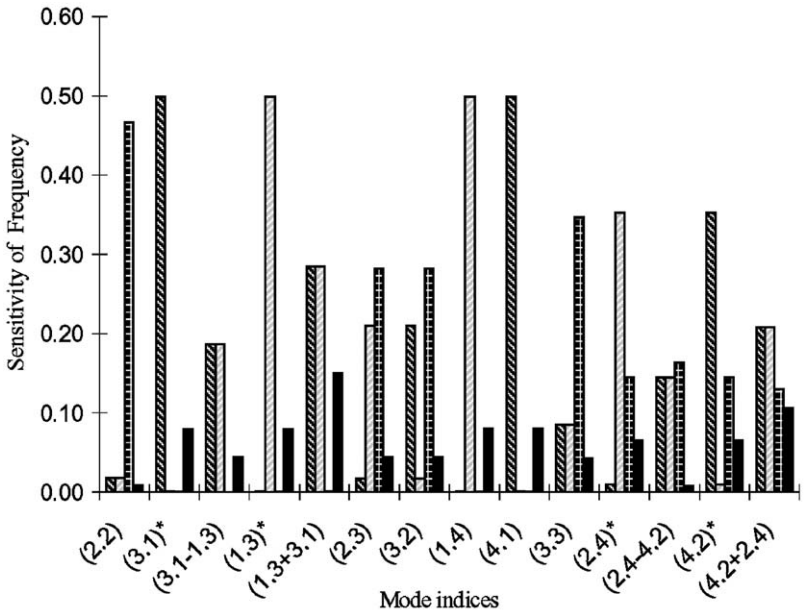

Fig. 1. Frequency sensitivities of the square SMC plate (* diagonal-mode-related pure mode): E_x; E_y; G_{xy}; ν_{xy} are engineering elastic constants.

Table 4
Plate frequency global fit data

FITTING OBJECTIVE: PLATE FREQUENCY MODE (2,2)
TOTAL FITTING POINTS = 1000
FITTING BASIC FUNCTION IS:-
FREQ = A1 + A2*X1 + …A8*X7 + A9*X1*X2 + … + A29*X6*X7 + A30*X1ˆ2 + … + A36*X7ˆ2
FITTING VARIABLES: X1 = L_x/L_y, X2 = H/L_y, X3 = E_x/E_y, X4 = G_{xy}/E_y,
X5 = G_{yz}/E_y, X6 = PNU_{xy}, X7 = DENSITY RATIO
THE VARIABLES XI ARE NORMALIZED
XMAX(I) = 4.000 0.2000 0.711 0.711 0.500 1.200
FITTING RESULT:
A1 = 0.52488 A2 = −0.32651 A3 = 8.51919 A4 = 0.00104 A5 = −0.87547 A6 = −0.49550 A7 = 0.95742
A8 = −0.41706 A9 = −1.51789 A10 = 0.00105 A11 = −0.14128 A12 = −0.02755 A13 = 0.00021 A14 = 0.06151
A15 = −0.02378 A16 = 2.02023 A17 = 0.21537 A18 = −0.00077 A19 = −0.82206 A20 = −0.00334 A21 = 0.00175
A22 = −0.00008 A23 = 0.00104 A24 = 0.09447 A25 = 0.00157 A26 = −0.23158 A27 = 0.00049
A28 = −0.01730 A29 = −0.00033 A30 = 06160 A31 = −6.80326 A32 = −0.00013 A33 = 1.96536 A34 = 0.64197
A35 = −1.59288 A36 = 0.13569
MAXIMUM RELATIVE ERROR (IMAX) = POINT 946; 2.216515071815996
SQUARE ERROR = 6.578719490706451D-03

The mode sequence is important for elastic characterization and damage assessment procedures because they basically rely on comparisons of test and computed frequency parameters, with a one-to-one correspondence from mode to mode. Table 2 shows plate aspect ratio and fiber

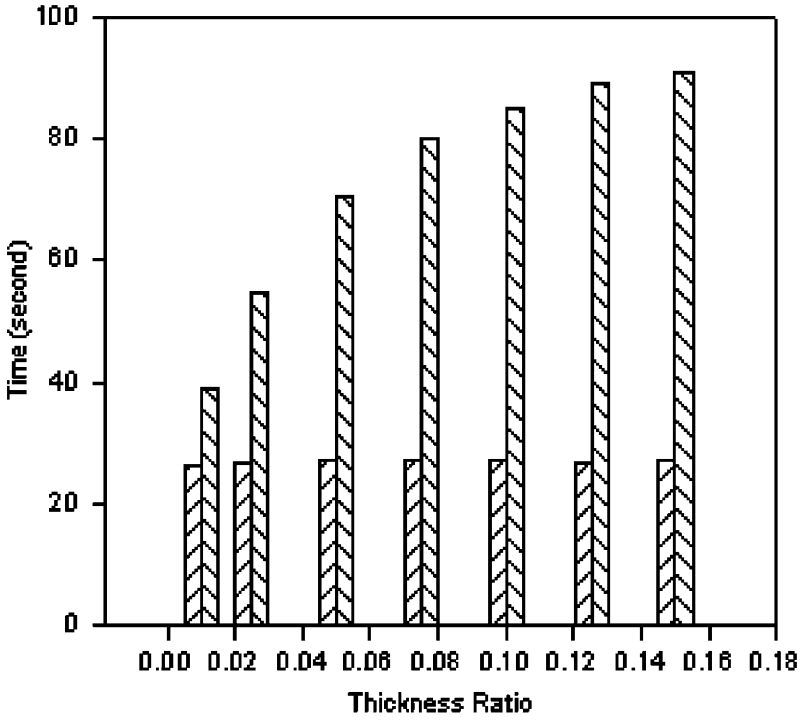

Fig. 2. Time of forward problem—graphite/epoxy: ▨, with library, ▨, without library.

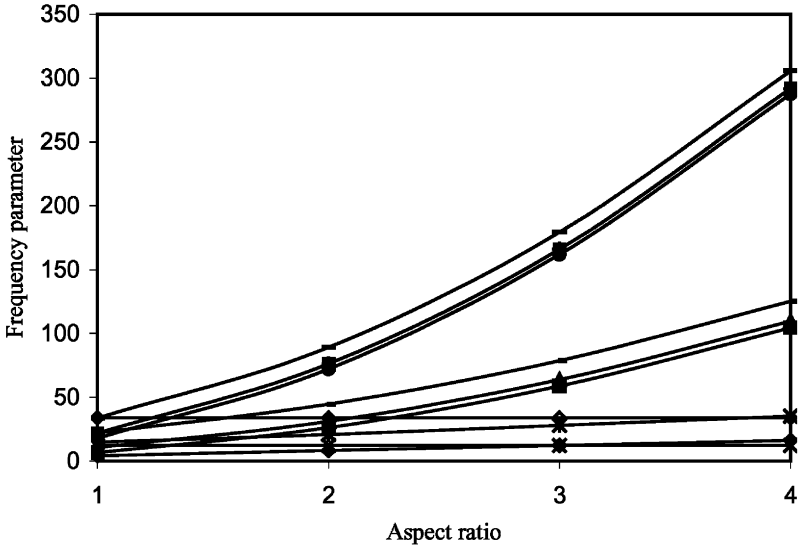

Fig. 3. Effect of aspect ratio on frequency parameter for glass/epoxy (angle = 0°): –◆– mode (2,2); –■– mode (1,3); –▲– mode (2,3); – × – mode (3,1); –✻– mode (3,2); –●– mode (1,4); –■– mode (2,4); —— mode (3,3); —— mode (3,4); —◇— mode (4,1).

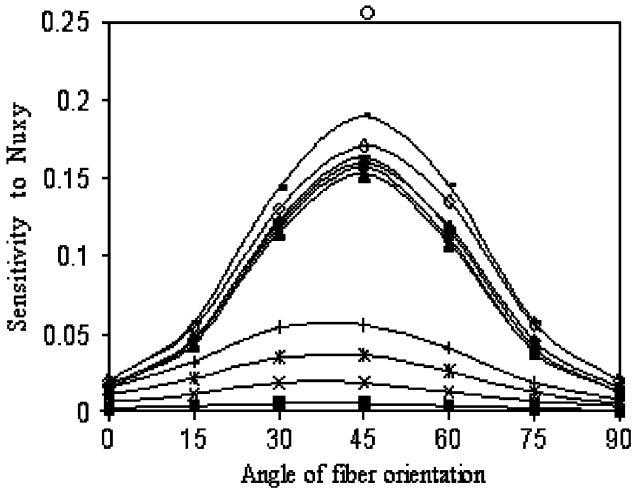

Fig. 4. Effect of fiber angular orientation on Poisson ratio sensitivity of glass/epoxy plate: –●– mode (3,1); –■– mode (2,2); –▲– mode (4,1); – × – mode (3,2); –✻– mode (4,2); –●– mode (5,1); —|— mode (5,2); —▬— mode (1,3); —▬— mode (6,1); —⊸— mode (2,3).

Table 5
Effect of experimental frequency error in high-sensitivity modes on predicted elastic constants

High-sensitivity mode for particular elastic constant		% Deviation from static values prediction (modal frequency in Hz)	
Mode (1,4) for E_y	0% (166.1 Hz)	6.5% (176.97 Hz)	13.53% (188.33 Hz)
Predicted elastic constant			
E_x (Gpa)	124.3	124.7	124.9
E_y (Gpa)	10.22	11.09 (+8.5%)	11.90 (+16.4%)
G_{xy} (GPa)	6.358	6.373	6.357
v_{xy}	0.21	0.20	0.21

orientation affecting the mode sequence. The gradual progression in mode sequence rearrangement from 0° to 45° is evident.

From the results, as exemplified by Fig. 1, although general rules do not yet appear inferrable, it would seem that modes that involve more deformation along a particular axis, such as (3,1) and (4,1) for the x-axis, tend to manifest higher frequency sensitivity of the relevant modulus, e.g. E_x. The sensitivity values for Poisson's ratio appear to be generally lower than for other elastic constants. This is probably one of the reasons why this constant is usually the most difficult to obtain accurately.

Table 3 shows the natural frequencies of a square SMC plate, under various approximations to the displacement function. It shows that our optimized three-mode representation gives answers of comparable accuracy to the 36-term Rayleigh–Ritz approach, while the optimized six-mode results are comparable in accuracy to the 64-term Rayleigh–Ritz, which is taken as the benchmark for all other solutions.

Fig. 1 shows the values of the sensitivity parameter obtained in the "forward" problem for the first ten modal frequencies inclusive of diagonal modes for the square SMC plate, as example. The results for the pure modes (1,3), (3,1), (2,4) and (4,2), are also presented to facilitate comparisons. It appears that the diagonal modes $(1,3 \pm 3,1)$ and $(2,4 \pm 4,2)$ are generally of higher sensitivities of frequency to each elastic constant than the pure modes. Thus inclusion of the diagonal modes would lead to better estimates of the elastic constants

Table 4 documents a typical attempt at global fit of the plate frequency data. The purpose of this exercise was to obtain a much faster solution to the forward and inverse problems by possibly generating interpolation tables for thick plate modal frequencies based on the geometric and material parameters (material density, orthotropy ratio, geometry, shear stiffness ratios, etc.) of the plate. The requirement for a method of speeding up the frequency computation for thick plates arises from the naturally longer computation times involved in solving the more complicated frequency equations for such plates. The table shows that this direct approach is not convergent, and not feasible. It gave inaccurate answers, and the parameter space was too wide. A solution method that breaks down the operation into a similar interpolation scheme for beam strips and then synthesizes the plate vibrations from those of the beams lying along the two orthogonal sides of the rectangular plate was however found to be quite successful, and a solution library for thick beam vibration was developed and used to obtain plate vibration results. Use of the library gives very accurate results for frequencies despite necessary interpolations and achieves very significant computation time savings—about 75–85% at 0.15 thickness ratio, were achieved, as shown in Fig. 2.

Plate aspect ratio is defined here as the ratio of the length of one side of the rectangular plate to the other, where the other one is being shortened gradually as the ratio goes from unity to four in the illustrative cases considered. This means that increasing aspect ratio essentially increases plate stiffness, hence resulting in the higher frequencies, as seen in Fig. 3. This was shown in our work to be typical, as it held true for the anisotropic materials considered (glass/epoxy and graphite/epoxy) as well.

It was also found that the frequency sensitivity of Poisson's ratio was about an order of magnitude less for graphite/epoxy than for glass/epoxy. The orthotropy ratios of these two materials are about 13.0 and 3.0, respectively. This probably suggests that it is more difficult to obtain an accurate Poisson's ratio for the higher orthotropy ratio, perhaps because of the increased difficulty of accurately obtaining strain in the two major directions. Fig. 4 shows maximum sensitivity of Poisson's ratio at 45°, in symmetrical profiles. This suggests that a 45° fiber-oriented sample would give better and more representative values of Poisson's ratio than other orientations, and this remains true as plate aspect ratio changes.

Further to the description in the results section, using the frequencies obtained and elastic constants predicted by using the static values of the elastic constants for graphite/epoxy as input to our characterization program, Table 5 shows that a 6.5% error in the E_y-sensitive frequency (4,1) results in an 8.5% error in E_y, while a 13.5% deviation in the (4,1) frequency leads to a 16.4% deviation in the predicted E_y value. This can be shown for other elastic constants and modal frequencies, and underscores the fact that even with a high fidelity characterization method, the predicted results can only be as good as the quality of the experimental data would permit. The referenced error data extracted from Table 5 can also be normalized with the input error in the frequency to yield relative errors. This means the relative errors are 1.3% and 1.2%

respectively. Frederiksen [14] plotted normalized parameter uncertainties for various plate aspect ratios (length-to-breadth) for the four elastic constants E_1, E_2, G_{12}, and v_{12}, using both the classical plate theory and a higher-order theory. For unity aspect ratio as in the present work, the normalized relative errors for the thin plate (using his Fig. 3) are about 0.8%, 1.1%, 1.6%, and 9% for E_1, E_2, G_{12}, and ν_{12}, respectively, and for the thick plate (using his Fig. 8) they are about 1.4%, 1.4%, 1.6%, and 10%, respectively. The present results compare favorably for the case considered. Grediac and his colleagues have steadily developed an approach christened the virtual fields method, which essentially utilizes the principle of virtual work to set up equations that link measured and desired quantities. The method has been applied to both static and dynamic test exercises. Grediac and Paris [16,36] utilized a direct identification method to obtain simulation [16] and experimental [36] results. They obtained bending stiffnesses, D_{ij}. For unidirectional graphite/epoxy, the simulation results for an input perturbation of 5–10% showed output modulus errors from less than 0.1% to about 3.8%. The actual experimental results showed modulus errors in the D_{ij} values from about 3% to 33%. This last value was for D_{12}, which represents Poisson's ratio. Grediac [43] also presented a method for the identification of invariant parameters governing the bending of anisotropic plates. In a numerical simulation, he perturbed the inputs up to 10% and obtained output errors ranging from 0.2% to 28.8%. Bledzki et al. [37] presented a similar direct method based on experimental design. For polyethylene-sized *E*-glass/epoxy composite, the percentage differences of the stiffness values they obtained by vibration over the static tensile values could be evaluated as–1.7% for E_1 and 43.1% for E_2. Grediac and co-workers also applied the virtual fields method to thick laminated tubes [38], and shear specimens [39]. In the latter work they observed that the transverse component stiffness Q_{xz} was more sensitive to strain measurement errors than others and that the accuracy of the method depended on the choice of fields and the numerical conditioning of the A matrix. They also concluded that, for the optical data acquisition method, which is one of the most practical for capturing large strain fields as required by this approach, errors due to strain measurement and evaluation, and coordinate errors of mis-centering the CCD camera do affect the results. Their simulations of 5% and 10% strain errors resulted in component stiffness error magnitudes of 1.3% and 2.5%, respectively. Their simulated coordinate mis-centering errors of 1 and 2 pixels, respectively, yielded component stiffness error magnitudes up to 4.2%. However, for Q_{xz}, which governs the Poisson's ratio, errors of 29% and 1800%, respectively, were recorded at eccentricities of 5 and 10 pixels, respectively.

Hwang and Chang [40] used a combination of commercial finite element and design of experiment computer programs to extract elastic constants. They considered several plates of varying rectangular plan dimensions. For carbon/epoxy plates, the percentage modulus deviations could be computed from their data to be 0.2–6.2% for E_1, 1.7–6.6% for E_2, 3.2–12% for G_{12}, and 8.7–52% for v_{12}. Grediac and co-workers further refined the virtual fields method for special fields, setting out the principles [41] and applying the method to in-plane problems [42]. The optimized special fields were chosen based on a minimization of a root sum square of the component stiffnesses Q_{ij}. For a test material, the modulus errors in the component stiffnesses ranged from zero to 9.7%.

From the diversity of results referenced, it could be seen that the results of the present work are very comparable with others.

6. Conclusion

The main factors affecting the use of a vibration-based method for elastic identification have been discussed. The basic analytical foundation of the method has been given, and the major factors that have bearing on the accuracy, economy and ease of use of the method have been identified as the inclusion or otherwise of the diagonal modes, where applicable, the frequency sensitivities of the elastic constants, the use of some effective scheme, such as a beam vibration interpolation library developed in our work, to expedite thick plate vibration analysis, as well as the plate aspect ratio, orthotropy ratio and reinforcing fiber orientation , as well as the goodness of the experimental data which serves as input to the identification or characterization procedure. A basic insight into how these important factors could affect the efficiency of the type of elastic characterization approach has been described here. Since most elastic characterization methods are posed as inverse problems that essentially match analytical modal data with their experimental counterparts, the factors highlighted in this paper should be applicable to a generic family of these methods.

Acknowledgements

The authors acknowledge the financial and other support of the ONR and Mechanics program officer Dr. Yapa D.S. Rajapakse, and also Wayne State University's Institute of Manufacturing Research for this research.

References

[1] American Society for Testing and Materials, *ASTM Standards And Literature Reference For Composite Materials*, ASTM, Philadelphia, PA, 1987.
[2] Automotive Composites Consortium, *Test Procedures for Automotive Structural Composite Materials*, A.C.C., Troy, MI, 1990.
[3] YU.V. Zelenev, L.M. Electrova, Determination of the dynamic parameters of polymer plates, *Soviet Physical Acoustics* 18 (1973) 339–341.
[4] J.A. Wolf, T.G. Carne, Identification of the elastic constants for composites using modal analysis, *Meeting of Society of Experimental Stress Analysis*, San Francisco, No. A-48, 1979.
[5] W.P. Dewilde, B. Narmon, M. Roovers, Determination of the material constants of an anisotropic lamina by free vibration analysis, *Proceedings of the Second Modal Analysis Conference*, Orlando, FL, 1984, pp. 44–49.
[6] L.R. Deobald, R.F. Gibson, Determination of elastic constants of orthotropic plates by a modal analysis/ Rayleigh–Ritz technique, *Journal of Sound and Vibration* 124 (1988) 269–283.
[7] P.S. Frederiksen, Identification of temperature dependence for orthotropic material moduli, *Mechanics of Materials* 13 (1992) 79–90.
[8] E.O. Ayorinde, R.F. Gibson, Y.-F. Wen, Elastic constants of isotropic composite materials from plate vibration test data, in: E.T. Camponeschi Jr. (Ed.), *Composite Materials: Testing and Design (Eleventh Volume)*, ASTM STP 1206, ASTM, Philadelphia, 1995, pp. 150–161.
[9] E.O. Ayorinde, R.F. Gibson, Elastic constants of orthotropic composite materials using plate resonance frequencies, classical lamination theory and an optimized three-mode Rayleigh formulation, *Composites Engineering* 3 (5) (1993) 395–407.

[10] E.O. Ayorinde, R.F. Gibson, Improved method for in-situ elastic constants of isotropic and orthotropic composite materials using plate modal data with trimodal and hexamodal Rayleigh formulations, *Journal of Vibrations and Acoustics* 117 (1995) 180–186.
[11] E.O. Ayorinde, On the sensitivity of derived elastic constants to the utilized modes in the vibration testing of composite plates, *Innovative Processing and Characterization of Composite Materials*, NCA-Vol. 20/AMD-Vol. 211, ASME, New York, 1995, pp. 55–64.
[12] E.O. Ayorinde, Elastic constants of thick orthotropic composite plates, *Journal of Composite Materials* 29 (1995) 1025–1039.
[13] E.O. Ayorinde, L. Yu, On the use of diagonal modes in the elastic identification of thin composite plates, *Journal of Vibration and Acoustics* 121 (1999) 33–40.
[14] P.S. Frederiksen, Parameter uncertainty and design of optimal experiments for the estimation of elastic constants, *International Journal of Solids and Structures* 35 (1998) 1241–1260.
[15] C.M. Mota Soares, M. Moreeira de Freitas, M. Araujo, P. Pedersen, Identification of material properties of composite plate specimens, *Composite Structures* 25 (1993) 277–285.
[16] M. Grediac, P.A. Paris, Direct identification of elastic constants of anisotropic plates by modal analysis: theoretical and numerical aspects, *Journal of Sound and Vibration* 195 (1996) 401–415.
[17] P.S. Frederiksen, Numerical studies for the identification of orthotropic elastic constants of thick plates, *European Journal of Mechanics A-Solids* 16 (1997) 117–140.
[18] P.S. Frederiksen, Natural vibrations of free thick plates and identification of transverse shear moduli, in: *Optimal Design with Advanced Materials*, Elsevier, Amsterdam, 1993, pp. 131–147.
[19] S.M. Dickinson, E.K.H. Lisd, On the use of simply supported plate functions in the Rayleigh–Ritz method applied to the flexural vibration of rectangular plates, *Journal of Sound and Vibration* 80 (1982) 292–297.
[20] C.S. Kim, S.M. Dickinson, Improved approximate expressions for the natural frequencies of isotropic and orthotropic rectangular plates, *Journal of Sound and Vibration* 103 (1986) 142–149.
[21] R.D. Mindlin, Influence of rotatory inertia and shear on flexural motions of isotropic, elastic plates, *Journal of Applied Mechanics* 1951 (1951) 51–58.
[22] T.J. Craig, D.J. Dawe, Flexural vibration of symmetrically laminated composite rectangular plates including transverse shear effects, *International Journal of Solids and Structures* 22 (1986) 155–169.
[23] K.M. Liew, Y. Xiang, S. Kitipornchai, Research on thick plate vibration: a literature survey, *Journal of Sound and Vibration* 180 (1995) 163–176.
[24] Lord Rayleigh, *Theory of Sound*, (2 Vols), Dover Publications, New York, 1945 (re-issue).
[25] G.B. Warburton, The vibration of rectangular plates, *Proceedings of the Institution of Mechanical Engineers* 168 (1954) 371–374.
[26] A.W. Leissa, The free vibration of rectangular plates, *Journal of Sound and Vibration* 31 (3) (1973) 257–293.
[27] R.D. Blevins, *Formulas for Natural Frequency and Mode Shape*, Van Nostrand, Princeton, NJ, 1979.
[28] P. Cawley, R.D. Adams, The location of defects in structures from measurements of natural frequencies, *Journal of Strain Analysis* 14 (1978) 49–57.
[29] J.J. Tracy, J.D. Dimis, G.C. Pardoen, The effect of impact damage on the dynamic properties of laminated composite plates. *Proceedings of the Fifth International Conference on Composite Materials*, San Diego, California, 1985, pp. 111–125.
[30] S.M. Dickinson, E.K.H. Li, On the use of simply supported plate functions in the Rayleigh-Ritz method applied to the flexural vibration of rectangular plates, *Journal of Sound and Vibration* 80 (2) (1982) 292–297.
[31] N.V. Banichuk, *Problems and Methods of Optimal Structural Design*, Plenum Press, New York, 1983.
[32] K.K. Choi, Design sensitivity analysis and optimization of built-up structures, Final Technical Report, October 1981–December 1986, Center for Computer Aided Design, College of Engineering, University of Iowa, 1986.
[33] K.D. Hjelmstad, M.R. Banan, Time-domain parameter-estimation algorithm for structural computation aspects, *Journal of Engineering Mechanics* 121 (3) (1995) 424–434.
[34] V.B. Hammer, M.P. Bendsoe, R. Lipton, P. Pedersen, Parametrization in laminate design for optimal compliance, *International Journal of Solids and Structures* 34 (4) (1997) 415–434.
[35] D.J. Dawe, O.L. Roufaeil, Rayleigh–Ritz vibration analysis of Mindlin plates, *Journal of Sound and Vibration* 69 (3) (1980) 345–359.

[36] M. Grediac, P.A. Paris, Direct identification of elastic constants of anisotropic plates by modal analysis: experimental results, *Journal of Sound and Vibration* 210 (6) (1998) 643–659.
[37] A.K. Bledzki, A. Kessler, R. Rikards, A. Chate, Determination of elastic constants of glass/epoxy unidirectional laminates by the vibration testing of plates, *Composites Science and Technology* 59 (1999) 2015–2024.
[38] F. Pierron, S. Zhavoronik, M. Grediac, Identification of the through-thickness properties of thick laminated tubes using the virtual fields method, *International Journal of Solids and Structures* 37 (32) (2000) 4437–4453.
[39] F. Pierron, M. Grediac, Identification of the through-thickness moduli of thick composites from whole-field measurements using the Iosipescu fixture: theory and simulations, *Composites Part A* 31 (2000) 301–318.
[40] S.-F. Hwang, C.-S. Chang, Determination of elastic constants of materials by vibration testing, *Composite Structures* 40 (2000) 183–190.
[41] M. Grediac, E. Touissant, F. Pierron, Special virtual fields for the direct determination of material parameters with the virtual fields method. 1—principles and definition, *International Journal of Solids and Structures* 39 (10) (2002) 2691–2705.
[42] M. Grediac, E. Touissant, F. Pierron, Special virtual fields for the direct determination of material parameters with the virtual fields method. 2—application to in-plane properties, *International Journal of Solids and Structures* 39 (10) (2002) 2707–2730.
[43] M. Grediac, On the direct determination of invariant parameters governing anisotropic plate bending problems, *International Journal of Solids and Structures* 33 (27) (1996) 3969–3982.